Stochastic Lagrangian Velocity Dynamics and Upscaled Transport in Rough Fractures

Alessandro Lenci, Yves Méheust, Marco Dentz, Vittorio Di Federico

alessandrolenci.com

MS08 – Mixing, dispersion and reaction processes across scales in heterogeneous and fractured media

Nantes, France | 22 May 2026

1. Motivation

Anomalous transport is a dynamical consequence of velocity intermittency

Spatially heterogeneous flow fields produce two coupled transport signatures:

- **Fast channelized pathways:** early arrivals and rapid plume spreading
- **Quasi-stagnant regions:** delayed advective motion and BTC tailing

This stochastic Lagrangian structure controls anomalous transport and must be retained in any predictive upscaled model.

Based on an arXiv preprint
under review in *JFM*

arXiv: 2510.07272

2. Geometry and Flow Dynamics in Geological Fractures

Geometry

Self-affine roughness generates heterogeneous aperture fields

$$a(\mathbf{x}) = h_\mathrm{u} - h_\mathrm{l} + a_\mathrm{m} \qquad \mathcal{F}(\kappa) \propto \kappa^{-(2+2H)}$$

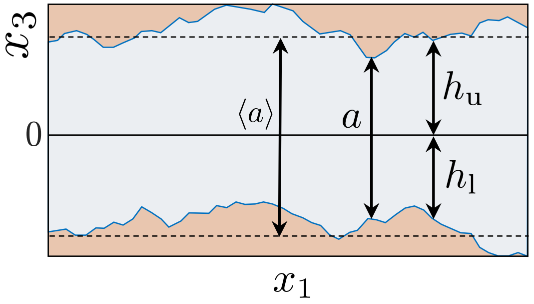

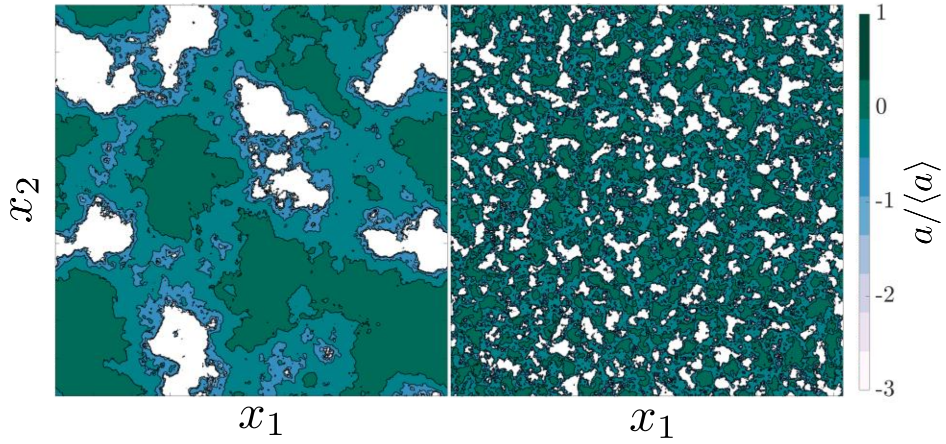

Aperture heterogeneity is controlled by:

- Closure $\sigma_a/\langle a \rangle$
- Correlation length

Flow model

2-D Depth-averaged flow governed by *Reynolds equation*

$$\nabla \cdot [a(\mathbf{x})^3 \nabla P] = 0$$

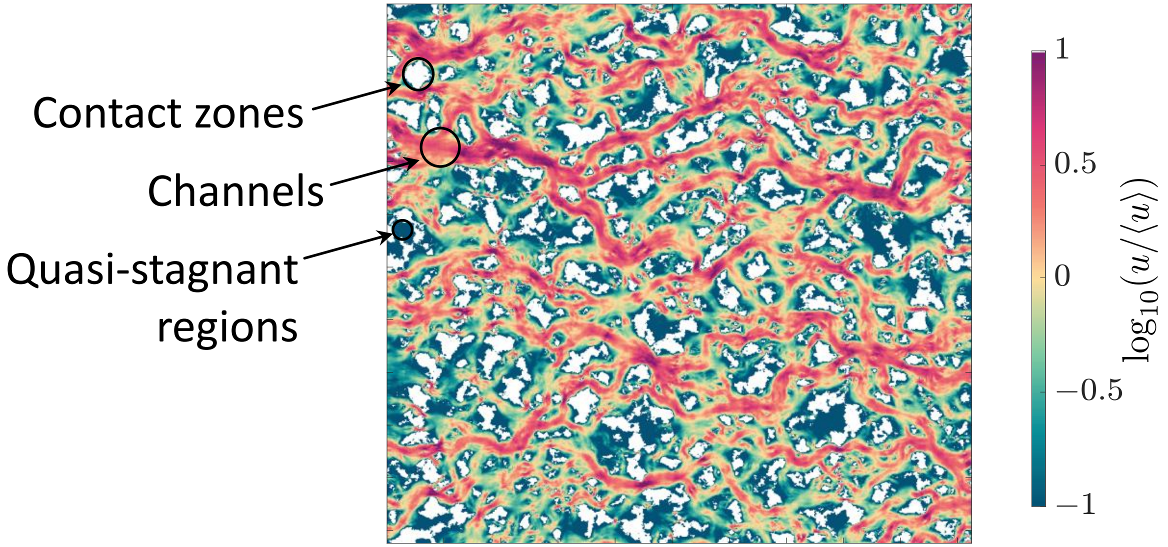

Local Transmissivity $\propto a(\mathbf{x})^3$

Aperture variability induces strong transmissivity contrasts, leading to channelized flow.

GEONEAT

InterPore

3. 2-D Reference Transport Model

Purely Advective Transport: $$\frac{\partial c(\mathbf{x},t)}{\partial t} = -\nabla \cdot \mathbf{u}(\mathbf{x}) c(\mathbf{x},t)$$

The 2D resolved reference model combines an upwind-weighted finite-volume discretization of advective transport with a recursive TDRW particle-tracking algorithm.

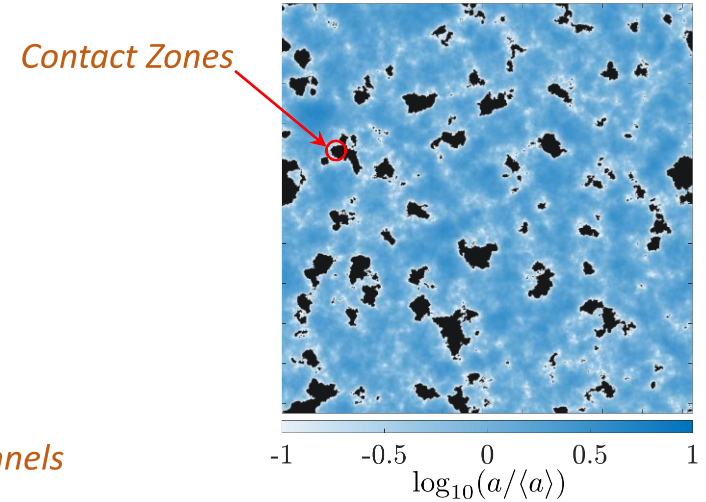

TDRW Random Walk Scheme

- Transition Probabilities $$w_{\parallel}^{(i,j)} = \frac{|u_1^{(i,j)}|}{|u_1^{(i,j)}| + |u_2^{(i,j)}|} \quad \text{and} \quad w_{\perp}^{(i,j)} = \frac{|u_2^{(i,j)}|}{|u_1^{(i,j)}| + |u_2^{(i,j)}|},$$
- Transition Time $$\tau^{(i,j)} = \frac{\Delta x}{|u_1^{(i,j)}| + |u_2^{(i,j)}|}$$

Recursive Algorithm

$$x_1^{(n+1)} = x_1^{(n)} + \xi^{(n)} \Delta x \frac{u_1((n))}{|u_1((n))|}, \quad x_2^{(n+1)} = x_2^{(n)} + (1-\xi^{(n)}) \Delta x \frac{u_2((n))}{|u_2((n))|} \qquad \mathrm{t}^{(n+1)} = t^{(n)} + \tau^{(n)}$$

TDRW is a residence-time formulation of purely advective transport on the resolved velocity field.

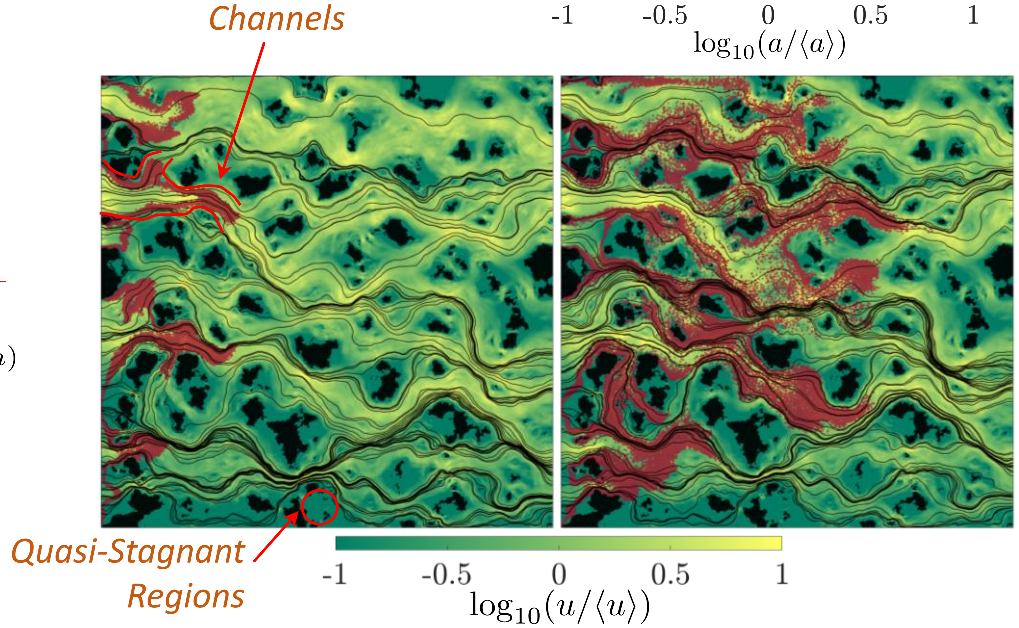

GEONEAT

InterPore

4. Upscaled 1-D Transport Model

1D upscaled kinematics: $$\frac{dx_1(s)}{ds} = \chi^{-1}, \quad \frac{dt(s)}{ds} = v_s(s)^{-1}$$

Tortuosity $\rightarrow$ $$\chi = \frac{\langle v_e \rangle}{\langle v_1 \rangle}$$

Coarse-grained formulation: $$x_{1,n+1} = x_{1,n} + \frac{\Delta s}{\chi}, \qquad t_{n+1} = t_n + \frac{\Delta s}{v_n}.$$

Transition model $\rightarrow$ v_n

Lagrangian velocity PDF $\rightarrow$ $f_s(v)$; *Eulerian velocity PDF* $\rightarrow$ $f_e(v)$

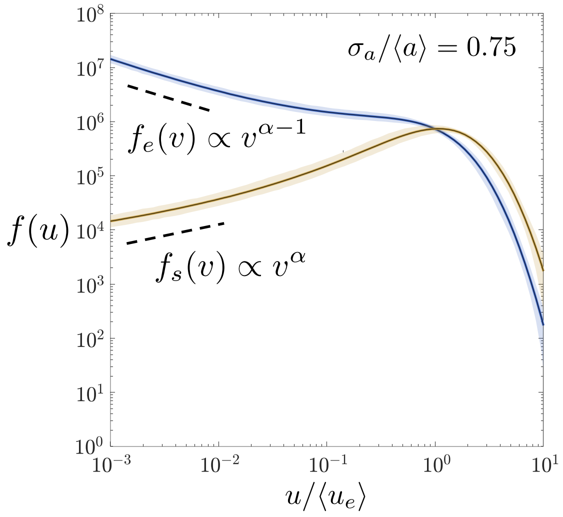

The Lagrangian velocity PDF is obtained by flux-weighting the Eulerian PDF: $$f_s(v) = \frac{v f_e(v)}{\langle v_e \rangle}$$

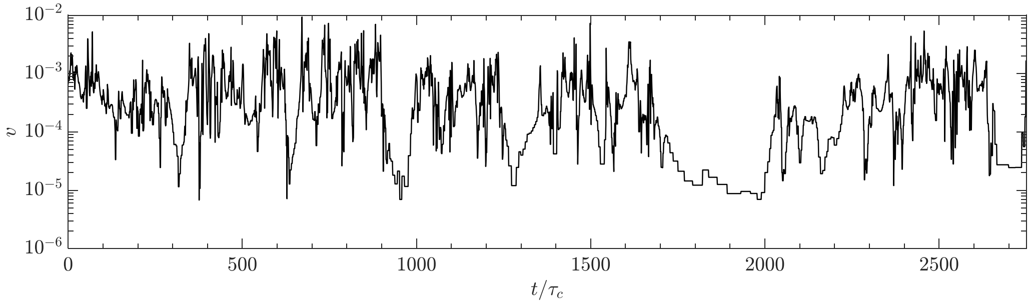

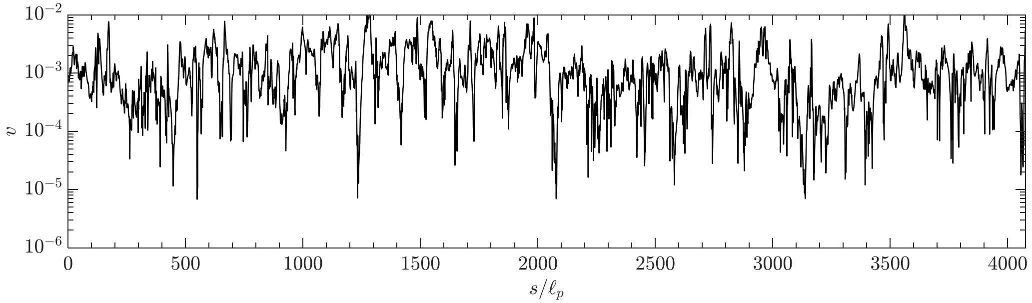

- The upscaled process acts in space: velocities are correlated along the streamline, while time is accumulated through residence times.
- Constant-space sampling isolates the spatial velocity sequence relevant for CTRW transitions.

Velocity heterogeneity becomes anomalous transport through spatial persistence and residence-time amplification.

5. Stochastic Velocity Transition Model

The transition model generates a spatially correlated sequence of Lagrangian velocities with prescribed stationary distribution $f_s(v)$ and persistence length ℓ_c.

Lagrangian Persistence Length

The **Ornstein–Uhlenbeck** process defines a stationary Gaussian Markov model for the normal-score velocity along the streamline.

Normal-score transform

$$w(s) = \Phi^{-1}\{P_s[v_s(s)]\} \qquad\qquad v_s(s) = P_s^{-1}\{\Phi[w(s)]\}$$

Ornstein–Uhlenbeck transition in space

$$w_{n+1} = w_n \left(1 - \frac{\Delta s}{\ell_c}\right) + \sqrt{\frac{2\Delta s}{\ell_c}}\,\xi_n$$

The OU model preserves the velocity PDF and spatial persistence, allowing the 1D model to reproduce anomalous spreading and BTC tailing.

6. Mean Displacement: plume drift and injection memory

Mean longitudinal displacement tracks the drift of the plume centroid.

At *early times*, particles retain the velocity statistics imposed at injection.

Flux-weighted injection oversamples high-velocity channels, producing a larger initial drift velocity.

At long times, both injection protocols converge toward the same linear regime as particles sample the stationary Lagrangian velocity distribution.

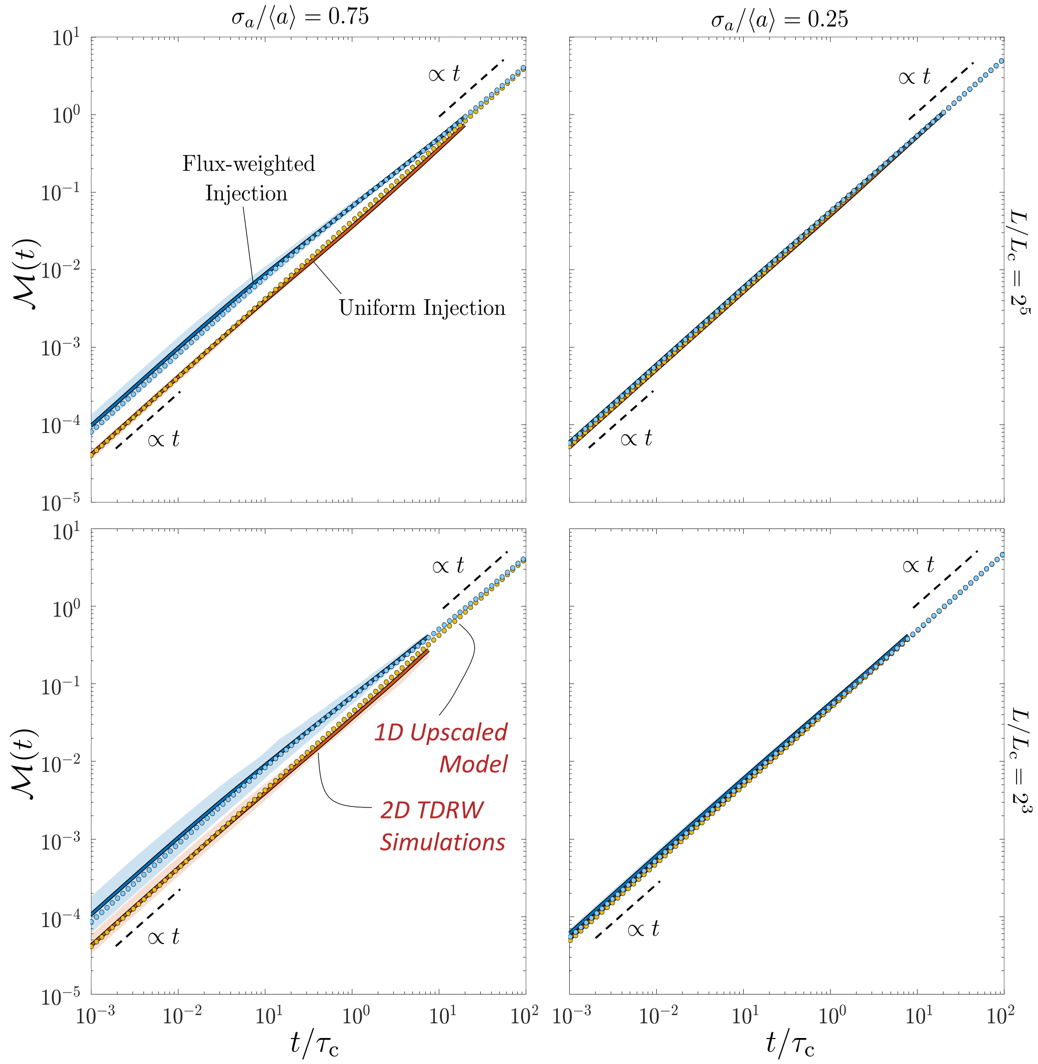

Mean displacement diagnoses injection-memory loss and convergence toward stationary advective sampling.

GEONEAT

InterPore

7. Displacement Variance: anomalous spreading

Particle displacement variance measures plume spreading around the centroid

Early time: ballistic spreading due to persistent initial velocity contrasts.

$$\mathcal{V}(t) \sim t^2$$

Late time: scaling controlled by the low-velocity tail of the Eulerian velocity PDF.

Strong closure produces broader low-velocity statistics and persistent superdiffusion.

$$\mathcal{V}(t) \sim t^{2-\alpha}$$

For weak heterogeneity, spreading approaches marginal anomalous behavior.

$$\mathcal{V}(t) \sim t \ln t$$

Variance growth is the clearest moment-based signature of anomalous transport, linking plume spreading to the low-velocity structure of the flow field.

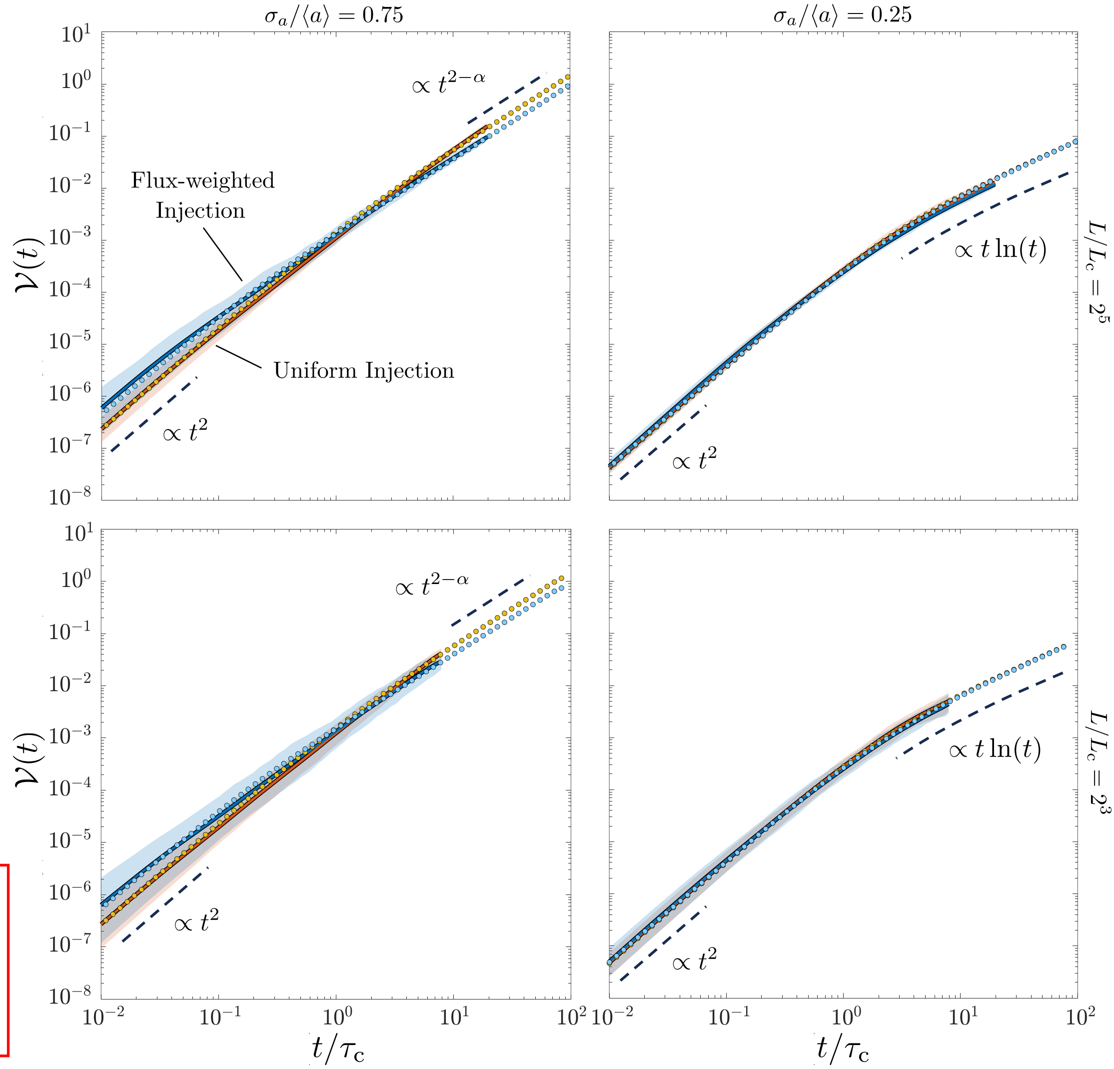

8. Breakthrough Curves: anomalous arrival times

BTCs describe the distribution of first-passage times at the fracture outlet

- Strong aperture heterogeneity broadens arrival-time distributions
- High-velocity channels control early arrivals and peak position
- Low-velocity regions control late-time power-law tailing
- Tail exponents follow from the low-velocity scaling $f_s(u) \sim u^{\alpha}$

Flux-weighted injection $\mathcal{F}(t) \sim t^{-2-\alpha}$

Uniform injection $\mathcal{F}(t) \sim t^{-1-\alpha}$

BTC tailing converts Lagrangian velocity intermittency into an observable outlet signal.

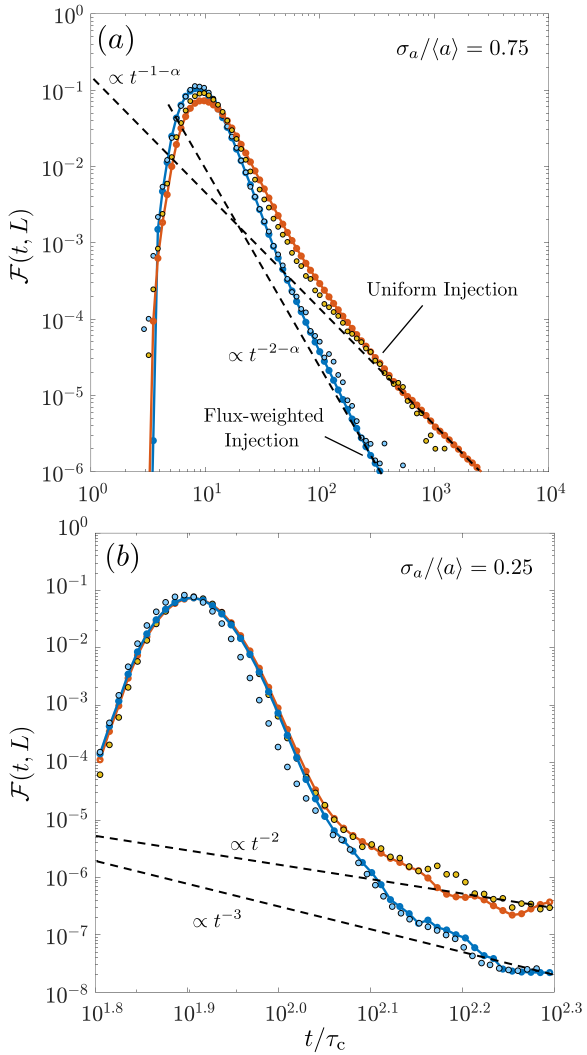

9. Conclusions

- Rough fracture geometry controls advective transport through flow channeling and low-velocity regions.
- Aperture-induced velocity intermittency produces non-Fickian spreading, visible in displacement variance and BTC tailing.
- Late-time scaling is governed by the low-velocity tail of the Lagrangian/Eulerian velocity statistics.
- The agreement between 2D TDRW and 1D CTRW indicates that the relevant information for upscaling is contained in the Lagrangian velocity statistics and their spatial persistence.

10. Acknowledgements

Supported by the European Union
Marie Skłodowska-Curie Actions (MSCA), **GEONEAT** Project (G.A. 101111216)

MARIE CURIE ACTIONS

Funded by the European Union

University of Bologna · Stanford University · Géosciences Rennes

ALMA MATER STUDIORUM UNIVERSITÀ DI BOLOGNA

Funded by the European Union. Views and opinions expressed are however those of the authors only and do not necessarily reflect those of the European Union or the European Commission. Neither the European Union nor the granting authority can be held responsible for them.

GEONEAT

InterPore

GEONEAT

Thank you for your attention

alessandrolenci.com

InterPore